JOURNAL OF MATERIALS SCIENCE 1 (1966) 127–141

Some Observations on Thin Magnetic Films made by Continuously Monitoring the Coercive Force

J. C. HENDY, H. D. RICHARDS, A. W. SIMPSON*
Allen Clark Research Centre, The Plessey Co Ltd, Caswell, Towcester, Northants, UK

Received 12 October 1965

1. Introduction

Thin ferromagnetic films are of interest from the standpoint of theoretical magnetism, and also because of their potential practical applications. Specially-prepared ferromagnetic films possessing uniaxial anisotropy, rectangular hysteresis loops and low coercive force, and characterised by a much faster switching mode for flux reversal than ferrite cores, can be used as storage elements in digital computers and control systems. The rectangularity of the hysteresis loops of thin ferromagnetic films and the variation of their intrinsic coercivity with thickness are dependent on the distribution of the magnetisation vectors, or the domain configuration, which in turn are influenced by the method of preparation and the chemical composition. Hence, detailed investigation of the domain configuration of ferromagnetic thin films as a function of the conditions of preparation, chemical composition and thickness, and a study of the behaviour of their domain structure in a magnetic field can be of help in choosing the most suitable and efficient elements for computer storage applications.

The structure of the domain walls in evaporated 80/20 Ni–Fe films is known to change as their thickness is varied. For very thin films *Néel walls* exist; in these, the magnetisation vector within the wall rotates in the plane of the film, as illustrated in fig. 1a. For thick films, the walls are of the *Bloch type* in which the magnetisation vector rotates out of the plane of the film (fig. 1b); this type of wall exists in normal bulk materials. In the intermediate range of thickness, a more complex wall structure is evident, in which the magnetisation vector periodically rotates out of the plane as well as in the plane of the film and has along its length a series of evenly-spaced Néel segments perpendicular to the main wall (as shown in fig. 1c). This is called a *cross-tie wall*. Hulyer [1] has investigated the domain structure in successively thicker films and has shown that the transition between each type of structure is not abrupt but can extend over a few hundred Ångströms in film thickness. He found that the transition from Néel to cross-tie walls extended from a film thickness of 150 Å to approximately 400 Å and that the transition from cross-tie to Bloch walls extends in thickness from approximately 900 Å to 1100 Å. He has also shown that the maximum number per unit length of wall of perpendicular Néel segments or cross-ties occurred at 800 Å. Methfessel, Middelhoek and Thomas [2, 3] have also made a study of the walls occurring in thin 80/20 Ni–Fe evaporated wedge films, and they also show that the maximum cross-tie density occurs at a film thickness of approximately 800 Å.

The experimental conditions in the work quoted above were not really ideal. In Hulyer's [1] work, arrays of 25 thin film disc-shaped samples were prepared by evaporation through a mask, and, for each evaporation, three batches with differing thicknesses were prepared. Consequently, the conditions of evaporation and substrate surface could vary throughout the experments. In the experiments described by Methfessel *et al* [2], the difficulties of reproducibility of the thin films were avoided by evaporating a wedge-shaped film so that the thickness tapered from a few Ångströms to 2000 Å in one evaporation. However, with this experiment there are

*Now at the Applied Sciences Laboratory, University of Sussex.

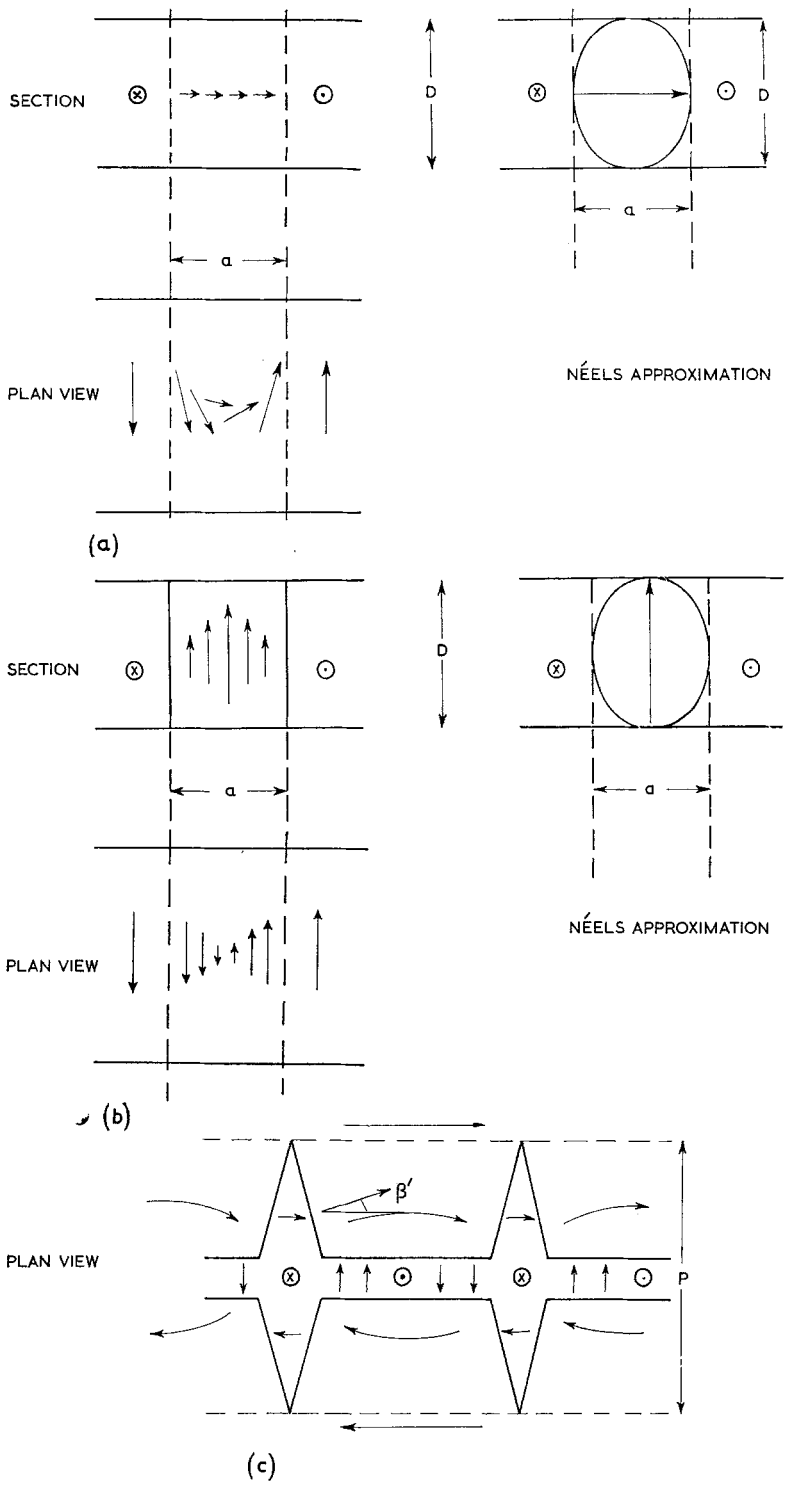

Figure 1 The domain wall models: (a) Néel wall model (section and plane view); (b) Bloch wall model (section and plane view); (c) cross-tie wall model (plane view). In each diagram the arrows represent components of the magnetisation vector in the plane of the paper. The diagram also shows the Néel approximation to the magnetisation within the section of the Bloch and Néel walls.

difficulties in accurately measuring the variation of coercive force with thickness. In order to avoid these complications a method of continually monitoring the coercive force during deposition was devised.

The initial objective of this work was to use the coercive force monitoring apparatus to make a more detailed investigation of the variation of coercive force with thickness, and in particular to establish this variation in the Néel wall region and compare it with theory. Measurements of the coercive force/thickness relationship of several nickel-cobalt-phosphorus alloys produced by electroless deposition have been made by continuously monitoring the coercive force during deposition, hence avoiding reproducibility problems. No attempt has yet been made to correlate these relationships with observations of domain structure, but anomalies in the relationships (see fig. 2) have been found which are similar to

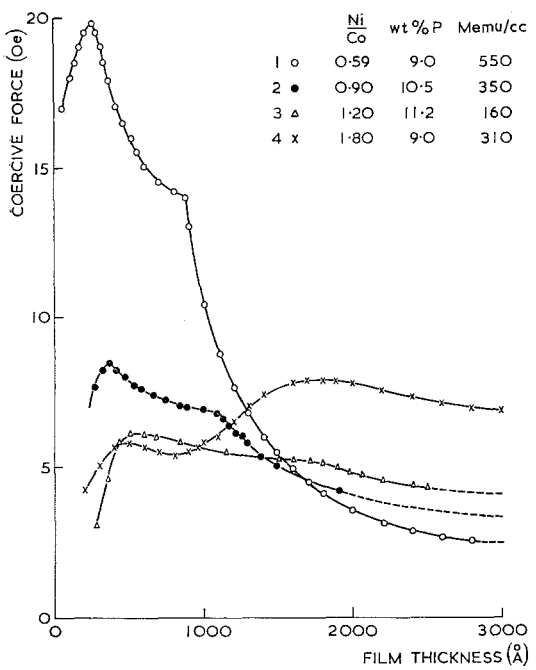

Figure 2 Some continually monitored coercive force/thickness relationships of Ni-Co-P films.

those found by Methfessel *et al* [2]. The thickness at which the anomalies occur are taken to be associated with the change of domain wall structure, and hence the exchange constant for the particular alloy may be evaluated. It has also been found that the coercive force/thickness relationship is a useful tool in evaluating the properties of new materials for use in computer storage applications. In addition, the technique can be used for studying the coupling phenomena [4, 5] between two ferromagnetic films which are separated by a thin non-magnetic layer.

2. Theoretical Introduction

Details of the domain structure in a magnetic material may be found by determining the domain configuration which has minimum total energy.

The total energy of a domain wall is the sum of the following terms: exchange energy; anisotropy energy (caused by crystal stress, or induced anisotropy); and magnetostatic energy associated with the free poles along the domain wall. The last term plays an important part in determining the variation of the direction of the magnetisation vector through the wall. When calculating the energy of a domain wall, Néel [6] avoided the complication of the continuous variation of the direction of the magnetisation vector within a domain wall by assuming that the centre of a wall is characterised by a uniform direction of magnetisation normal to the magnetisation in the adjoining domains. Within a Bloch wall, the magnetisation vector is normal to the plane of the film, and, for simplification, Néel assumed the wall to have an elliptical cross-section with its long axis (parallel to the magnetisation) corresponding to the film thickness, D (see fig. 1b), while its short axis is associated with the wall width, a. The magnetostatic energy E_m per cm^2 of a Bloch wall is associated with the demagnetising field and given by

$$E_m = \tfrac{1}{2}(NM)\,(aM)$$

where $N = \dfrac{4\pi a}{a + D}$ and M is the saturation magnetisation. Therefore

$$E_m = \frac{2\pi a^2 M^2}{(a + D)}$$

For a 180° Bloch wall which is parallel to the easy axis of magnetisation, the magnetisation direction is defined by the expression

$$\phi = \pi\left(\frac{x}{a}\right) \text{ for } \frac{-a}{2} \leqslant x \leqslant \frac{a}{2}$$

where ϕ is the angle between the magnetisation vector and a direction in the plane of the wall

perpendicular to the plane of the film. The exchange energy E_A is given by

$$E_A = A\left(\frac{d\phi}{dx}\right)^2 = \frac{A\pi^2}{a^2}$$

in which A is the exchange constant. The mean anisotropy energy density is given by

$$E_K = \frac{1}{a}\int_{-a/2}^{+a/2} K\cos^2\phi \, dx = \tfrac{1}{2}K$$

in which K is the anisotropy constant.

Middelhoek [7] has extended these calculations for finding the energies of Bloch, Néel and cross-tie walls per unit area of the wall; these are shown below. In these calculations he has assumed the average magnetisation through a Bloch or Néel wall to be equal to the rms of the saturation magnetisation, which is a better approximation than the one used above in calculating the stray field energy of the wall.

Middelhoek's results for the energy γ of the three types of walls are as follows:

$$\gamma_{\text{BLOCH}} = \gamma_B = \frac{\pi^2 A}{a} + \frac{aK}{2} + \frac{\pi a^2 M^2}{(a+D)} \quad (1)$$

$$\gamma_{\text{NÉEL}} = \gamma_N = \frac{\pi^2 A}{a} + \frac{aK}{2} + \frac{\pi a D M^2}{(a+D)} \quad (2)$$

$$\begin{aligned}\gamma_{\text{CROSS-TIE}} = \gamma_{CT} &= \gamma_N(1-\sin\beta)^2 \\ &+ \gamma_N(1-\cos\beta)^2 + pK\sin^2\beta \\ &+ pE_\beta \sin^2[\beta - \pi/8] \\ &+ \pi D M^2 \sin^2\beta\end{aligned} \quad (3)$$

where E_β is a constant and p is the length of the cross-ties, and also to simplify the model the distance between successive cross-ties, and β is the average value of β' (see fig. 1c) and, therefore, represents the average value of the direction of magnetisation between the cross-ties. Middelhoek estimated that the average direction of the magnetisation between the cross-ties, β, to be $\pi/8$, if $E_\beta \gg K$, which is not an unreasonable assumption for thin films with low anisotropy.

By minimising the cross-tie wall energy with respect to the cross-tie length the following expression was found:

$$p = \frac{1.56\,\gamma_N - \pi D M^2}{K} \quad (4)$$

showing that the length of a cross-tie varies inversely as the anisotropy constant. The minimum value of the Néel wall energy in equation 2 with respect to the width is

$$\gamma_N = 2\pi^{\frac{1}{2}} M\sqrt{A} - \frac{\pi^2 A}{D}$$

Therefore substituting in equation 4,

$$p = 1.56\pi \frac{\left(2\pi^{\frac{1}{2}} M\sqrt{A} - \frac{\pi A}{D} - \frac{DM^2}{1.56}\right)}{K} \quad (5)$$

This expression for the cross-tie length has a maximum and the thickness at which this occurs is given by

$$Dp_{\max} = 2.33\frac{\sqrt{A}}{M} \quad (6)$$

By substituting the value of p from equation 5 into 3 when $\beta = \pi/8$ the cross-tie wall energy can be expressed as a fraction of the Néel wall energy and is given by

$$\gamma_{CT} = 0.61\gamma_N$$

By minimising the wall energies with respect to the wall width, the critical film thicknesses, D, for the transition between wall structures can be evaluated to the first approximation. For the transition from Néel to cross-tie walls this critical thickness is given by

$$D_{\text{N-CT}} = 0.89\frac{\sqrt{A}}{M} \quad (7)$$

and for the transition from cross-tie to Bloch walls by

$$D_{\text{CT-B}} = 7.43\frac{\sqrt{A}}{M} \quad (8)$$

It is interesting to note that the expressions for the three critical thicknesses given in equations 6, 7 and 8 are all in terms of the parameter $\sqrt{A}/M$ and, therefore, the ratio between any two of these critical thicknesses are independent of the fundamental magnetic properties of the film. Two ratios may be defined to roughly check the theory; a convenient pair of ratios are

$$R_1 = \frac{D_{\text{CT-B}}}{Dp_{\max}} = 3.33 \text{ and } R_2 = \frac{Dp_{\max}}{D_{\text{N-CT}}} = 2.50 \quad (9)$$

Substituting the value of the exchange constant for 80/20 Ni–Fe, 10^{-6} ergs/cm, and the saturation magnetisation, 800 emu/cm^3, into expressions 6, 7 and 8, the critical thicknesses, $D_{\text{CT-B}}$, $Dp_{\max}$ and $D_{\text{N-CT}}$, can be evaluated as 110 Å, 280 Å, 930 Å, respectively. At the critical thicknesses, $D_{\text{N-CT}}$ and $D_{\text{CT-B}}$, the cross-tie length should be zero. Putting $p = 0$ in equation 5 yields the thicknesses at which this occurs as

140 Å and 600 Å, which do not agree with the thicknesses evaluated from equations 7 and 8. However, the value of β assumed in equation 3 has a very critical effect on this result and if the value were chosen to be 19.1° instead of $\pi/8$ (22.5°), the calculated critical thicknesses for D_{N-CT} and D_{CT-B} (when $p = 0$) are 130 Å and 750 Å and from the corrected expression 7 and 8 are 110 and 750 Å, respectively. These thicknesses are more in keeping with Hulyer's results.

Only a little information is available on the influence of domain wall structure on the coercive force/thickness relationship. Some workers [2] have shown that for evaporated 80/20 Ni–Fe a maximum in coercive force occurs at a thickness which corresponds to the maximum cross-tie density, and that a point of inflection in the relationship occurs at a higher thickness which is associated with the transition from cross-tie to Bloch walls. However, these measurements were made on wedge-shaped films so that an exact correlation of coercive force with film thickness is difficult, especially in the transition region between wall structures.

A theoretical estimate of the thickness dependence of coercive force in the Bloch wall region has been made by Néel [8]. He assumed the surface of the film to have a finite roughness, and found the coercive force to be proportional to $D^{-4/3}$. Middelhoek [9] has extended these calculations to all wall structures. He assumes that if local thickness variations alone are considered to be the cause of domain wall coercive force, then for 180° walls, equating the change in wall energy to the change in magnetisation energy, i.e.

$$\mathrm{d}(\gamma\, Dl) = 2HMl\, D\mathrm{d}x$$

where H is the applied field, $\mathrm{d}x$ the distance moved by the wall and l the length of the wall (which he assumed to be constant), then the coercive force H_c is given by the above expression when the change of wall energy with distance is a maximum

$$H_c = \frac{1}{2MD}\left\{\frac{\partial\,(\gamma D)}{\partial x}\right\}_{\max}$$

Expanding this expression

$$H_c = \frac{1}{2M}\left\{\frac{\partial\gamma}{\partial D} + \frac{\gamma}{D}\right\}\left(\frac{\partial D}{\partial x}\right)_{\max} \qquad (10)$$

Using equation 10 the coercive force for Bloch walls may be evaluated as

$$H_{c_B} = 4.2\left(\frac{A^2}{M}\right)^{\frac{1}{3}} D^{-4/3}\left(\frac{\partial D}{\partial x}\right)_{\max} \qquad (11)$$

and if the thickness variations are assumed to be sinusoidal with an amplitude equal to the wavelength $\left(\frac{\partial D}{\partial x}\right)_{\max} = 1$. This result agrees with that calculated by Néel. Middelhoek has also found an expression for the coercive force of Néel walls, using equation 10, and found it to be independent of film thickness. However, one of the present authors disagrees [10] with this result and has found it to be dependent on D^{-1}; likewise, he has found the coercive force of cross-tie walls to be also dependent on D^{-1}.

The coercive force at D_{CT-B} can be calculated by substituting the value from equation 8 and equation 11. This gives

$$H_{c_{CT-B}} = 0.29M\left(\frac{\partial D}{\partial x}\right)_{\max} \qquad (12)$$

Richards [10] has shown that the coercive force for the transition between Néel and cross-tie walls is also proportional to the saturation magnetisation of the film.

3. Experimental Procedure

The materials chosen for investigation were films of nickel-cobalt-phosphorus alloys prepared by electroless deposition on to glass substrates. The first electroless plating solution used was that suggested by Heritage and Walker [11]. It contained nickel sulphate and cobaltous sulphate with hypophosphorous acid as the reducing agent, sodium citrate and ammonium sulphate as a buffer and was operated at 84° C at a pH of 9 ± 0.2.

Preliminary treatment of the substrates, which measured 10 cm × 7.5 cm, consisted of cleaning in a dilute ammonium fluoride etching solution, sensitising in 0.1% stannous chloride solution and activating in 0.01% palladium chloride solution, with thorough rinsing after each stage. All these solutions were used at room temperature, and the only critical factor was the pH of the palladium chloride solution, which had to be greater than 3, otherwise the activation efficiency varied over the substrate area and in some regions no deposit was formed. The patchy appearance of the initial deposit showed that absolutely uniform activation was not obtained; film thickness variations due to non-uniform activation averaged ± 50 Å.

Thickness variations resulting from the plating procedure itself were found to be negligible provided that plating rates below 150 Å/min were used. These were achieved by reducing the temperature of the plating bath to 54° C, the lowest temperature at which satisfactory plating could be obtained.

Films with nickel/cobalt ratios ranging between 0.6 and 2.2 and phosphorus contents ranging from 9 wt % to 12.5 wt % were obtained by varying the ratio of nickel to cobalt ions in the solution between 0.33 and 1.34 and by using a pH range of 8.0 to 9.0. At the low pH values the buffer properties of the solution became poor and it was necessary to add dilute ammonium hydroxide during the plating to maintain the desired conditions. Alteration of the buffer materials, particularly the sodium citrate, which also acts as a chelating agent, causes complex changes in the plating process and was not attempted.

All the films made were stressed and, if allowed to reach thicknesses in excess of 3000 Å, either blistered badly or became completely detached from the substrate. No evidence has been found of any chemical link between the films and glass surfaces and it is assumed that adhesion is due entirely to van der Waals forces.

When the film is to be used as a computer storage element the uniaxial anisotropy of magnetisation in the plane of the film, which is a necessary requirement, is normally provided by depositing the films in a uniform static field of 22 Oe provided by a large Helmholtz pair. It was found, however, that the replacement of the static field by a 50 c/sec alternating field of the same amplitude gave the same degree of alignment and other film properties. (For some film compositions the alignment was very good with the skew angle less than $\frac{1}{2}°$ and the dispersion of the easy axis less than $\pm 1°$.) Using an alternating field, the coercive force of the thin films can be monitored during deposition if an insulated coil is wound around the substrate holder (see fig. 3), so that longitudinal flux changes produced by the alternating aligning field may be sensed. Plenty of room must be allowed for the solution to flow through the coil to prevent any variation of film parameters under the coil itself; a gap of roughly 2 cm was used. The voltage generated across the sense coil is largely due to the applied alternating field; by placing a backing-off coil outside the Helmholtz pair in series opposition to the sense coil the unwanted voltages due to field changes can be eliminated, leaving only the voltage due to flux changes. The simple circuit shown in fig. 3 was used for displaying the hysteresis loops and the rate of change of flux against applied field on a cathode ray oscilloscope. The *RC* network shown in fig. 3 was used to correct any phase errors. Integration of the sense waveform was not satisfactory at very low film thicknesses because of the low signals involved, consequently the coercive force was taken to be proportional to the distance between the half-area points of the voltage transients. Generally the transients were symmetrical and therefore the distance between the peaks could be taken. Calibration of the oscilloscope thus gave the coercive force.

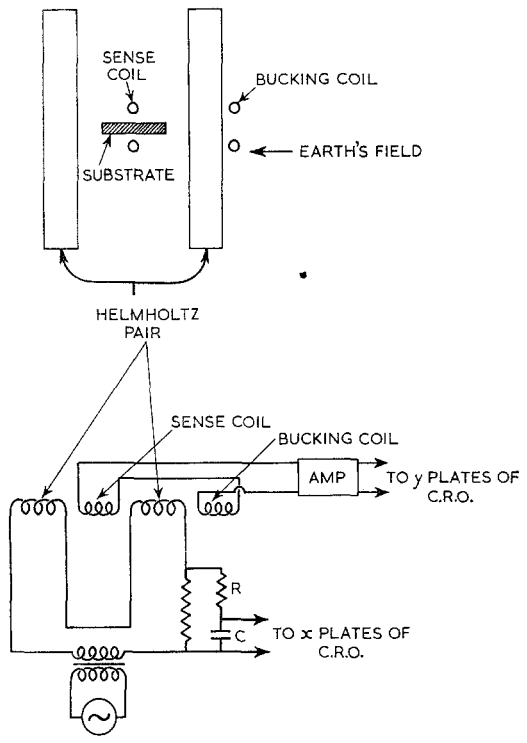

Figure 3 Experimental arrangement and circuit for continuously monitoring the coercive force.

The thicknesses of the films were measured using a surface profile measuring instrument (Talysurf, Taylor-Hobson) which can measure to $\pm$ 25 Å. Plating films for different times from the same solution confirmed that the plating rate was linear with time. Thus, if the plating rate is known, the monitored coercive force/plating time relationships can be converted to a

coercive force/thickness relationship, typical instances of which are plotted in fig. 2.

The chemical analyses of films plated to different thicknesses showed negligible changes in composition. Therefore, the saturation magnetisation of the material could be measured from a thick film using a calibrated hysteresis loop plotter.

Photographs were taken of the oscilloscope displays of the variation of rate of change of flux with field and tracings made from these photographs. Two typical sets of tracings are shown in fig. 4.

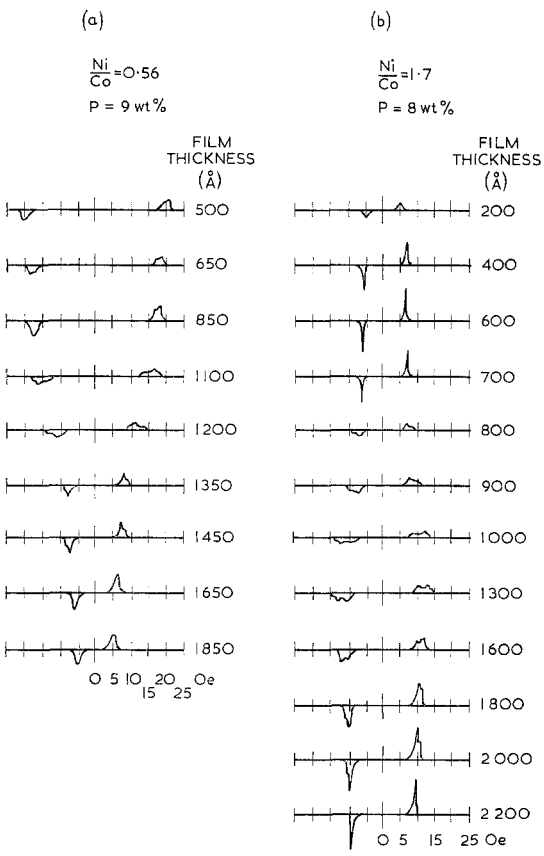

Figure 4 Tracings taken from photographs of two typical oscillographs of the rate of change of flux for an applied field at 50 c/sec.

4. Results

4.1. The Coercive Force/Thickness Relationship of some Ni-Co-P Alloys

Some curves of the coercive force/thickness relationship for different chemical compositions are shown in fig. 2 (the compositions and saturation magnetisations are shown in the insert). Starting at the high thickness end of the curves, the coercive force is seen to increase with decreasing film thickness, which was indicated by Néel's theory for Bloch walls in equation 11. As the film thickness is further reduced, films 1, 2 and 3 of fig. 2 show a point of inflection, and then a further increase in coercive force occurs until a maximum value is reached. All the films deposited showed such a maximum. The coercive force then decreases with decreasing thickness owing to the onset of superparamagnetism [12] (because the film becomes discontinuous, with the development of an isolated island structure). However, in film 4, which has a considerably higher nickel content, the maximum coercive force occurs at a greater thickness (1800 Å) and in this case observations below the maximum were possible. The curve shows that as the film thickness is decreased still further a second subsidiary maximum is observed before the film deteriorates into an island structure. It is possible that this phenomenon would be observed in films 1, 2 and 3 providing the film was continuous from the start, and it is surmised that a general relationship exists for the thickness dependence of the coercive force for the compositions studied. This general relationship is shown in fig. 5 where the thicknesses for the subsidiary maximum, minimum, maximum and point of inflection are denoted t_1, t_2, t_3 and t_4 respectively. For the whole range of alloys studied it was observed that the ratios t_3/t_2 and t_4/t_3 were 2.3 $\pm$ 0.2 and 3.1 $\pm$ 0.2 respectively. Now it was shown in the introduction that the theoretical ratios R_1 and R_2 of equation 9 related to the ratios of critical thickness for transition between different types of domain wall structures were 3.33 and 2.5 respectively. Therefore, since there is close agreement between the experimental ratios and the theoretical ratios, it can be said that:

$$D_{\text{N-CT}} = t_2;\ Dp_{\max} = t_3;\ D_{\text{CT-B}} = t_4$$

From now on t_2, t_3, t_4 will be used in discussing the experimental data. The thickness t_4 was clearly defined in alloys with high cobalt contents and low phosphorus contents, and the thickness t_2 only shown in alloys of high nickel content. More detailed investigation of the change of coercive force in the regions t_2 and t_4 was carried out by observing the oscillographs during deposition of alloys corresponding

to film 1 and film 4 (fig. 2), and the results are shown in fig. 4 for different film thicknesses.

Fig. 4a shows the observed rate of change of flux with field as a function of film thickness for an alloy nominally the same as film 1 (fig. 2). The figure clearly shows broadening of the voltage transients between 850 Å and 1350 Å. For this film, the value of t_4 is approximately 870 Å. It therefore seems that the thickness at which the point of inflection occurs is associated with a distinct change in wall movement process. The tracings for thicknesses less than 850 Å and greater than 1350 Å show one peak in each transient. However, as the film thickness is increased a subsidiary peak occurs at a lower field level than the main peak, as is shown in the drawing for a thickness of 1100 Å in fig. 4a. This peak then grows with increasing film thickness, and at the same time the main peak decreases in height. Therefore, it can be surmised that the broadening of the transient occurs because the film thickness variations allow the two types of wall to co-exist in the film. This effect is shown by the dotted lines in fig. 5. The form of the coercive force/thickness relationship is similar to that found by Methfessel *et al* [2] for 80/90 Ni–Fe when a transient from cross-tie walls to Bloch walls occurs.

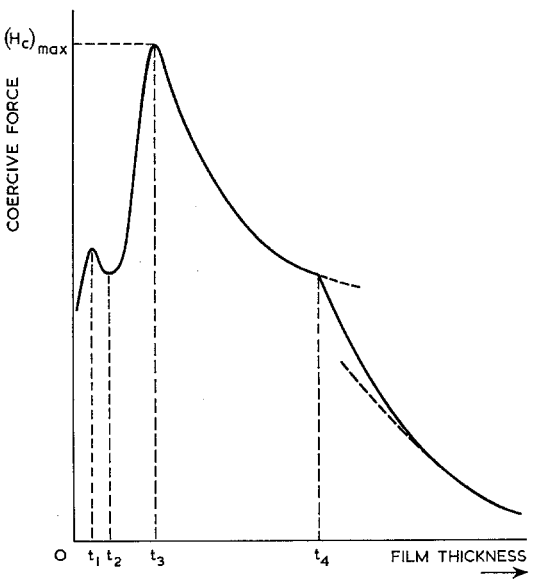

Figure 5 A surmised general form of the coercive force/thickness relationship.

Fig. 4b shows tracings of the rate of change of flux with field versus film thickness for an alloy of the same composition as film 4 (fig. 2). These results show a broadening of the transient between 700 Å and 1600 Å, that is for thicknesses between t_2 and t_3. This broadening can, therefore, be said to be associated with the coexistence of Néel and cross-tie walls in the film due to thickness variations. This was also observed by Hulyer in evaporated nickel-iron films, where he found that along a Néel wall irregular spacings of cross-ties occurred. From these results it may be surmised that the complete transition from Néel to cross-tie walls does not occur until the coercive force maximum at t_3 is reached.

4.2. Calculation of Exchange Constant from the Coercivity/Thickness Relationship

If the saturation magnetisation, M, and the critical film thicknesses, t_3 and t_4, are known, expressions 6 or 8 enable the value of the exchange constant to be calculated. For nickel-cobalt-phosphorus alloys with a constant phosphorus content of 9 wt %, the exchange constants obtained for films with nickel/cobalt ratios of between 0.55 and 1.5 were found to be roughly constant and to have a value of $3.3 \pm 0.4 \times 10^{-7}$ erg/cm. Fig. 6 shows the calculated exchange

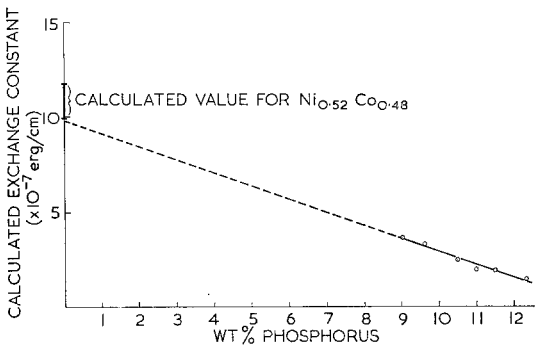

Figure 6 Variation of the exchange constant with phosphorus content in electroless-deposited Ni-Co-P films for a constant weight ratio of Ni/Co of 1.1.

constant from expression 6 versus phosphorus content for an alloy of constant nickel/cobalt ratio of 1.1. If the graph is extrapolated to zero phosphorus content, a value for the exchange content for pure 52/48 nickel-cobalt alloy of $1.1 \pm 0.1 \times 10^{-6}$ erg/cm is obtained. The exchange constants for pure cobalt and pure nickel have been measured [13, 14] at 20° C using spin wave resonance and found to be $1.3 \pm 0.08 \times 10^{-6}$ erg/cm and $7.5 \pm 0.75 \times 10^{-7}$ erg/cm, respectively, which, if a weight average is taken,

predicts an exchange of 1.0×10^{-6} erg/cm, in good agreement with the observed value. (The exchange constant may also be calculated more accurately from the expression given by Kittel [15] where

$$A = \frac{3KST_c}{Z(S+1)b}$$ and T_c = Curie temperature, b = lattice parameter

Using this expression and the values of T_c and b published for binary Ni–Co alloys by Hansen [16] and evaluating the constants by substitution for the quoted values of pure cobalt and pure nickel, the value for 52/48 nickel-cobalt may be calculated as $1.08 \pm 0.08 \times 10^{-6}$ erg/cm.) The presence of phosphorus in the deposited films causes them to have a very small grain size (less than 10 Å) which appears to be amorphous upon examination by electron diffraction methods. Analysis of the electron diffraction patterns is not conclusive, but does suggest that the nickel-cobalt alloy occurs in solid solutions with phosphorus rather than as phosphides, and therefore it is expected that the exchange constant will decrease, as observed, with increase in phosphorus content, due to an increase in the atomic spacing of the magnetic elements.

4.3. Coercive Force

Fig. 2 shows that the coercive force/thickness dependence of electroless nickel-cobalt-phosphorus alloys is a reciprocal law between t_1 and t_2, and between t_3 and t_4, and an inverse 4/3 power law above t_4, in good agreement with theory. More detailed results and comments are given elsewhere [10]. Quantitative agreement with theory is not obtained, however, unless $\left(\frac{\partial D}{\partial x}\right)_{max}$ in equation 10 is taken to be very much less than unity, which may be the case in electroless thin films which are extremely flat over an area of a few microns. The result for the variation of coercive force between t_3 and t_4 is in disagreement with the results obtained by Methfessel *et al* [2]; they found a maximum in coercive force to occur at the maximum cross-tie density, which should correspond to the critical thickness, t_4. The value of the coercive force at t_4 (see fig. 2 and insert) has been found to be roughly dependent on the saturation magnetisation in agreement with equation 12. Fig. 7 shows the variation of the maximum coercive force (occurring at t_3) as a function of phosphorus content for an alloy of constant nickel/cobalt ratio. The figure also shows the value of remanent induction as a function of phosphorus content, so that it can be shown that the coercive force at t_3 is approximately linearly dependent on the saturation magnetisation as indicated theoretically.

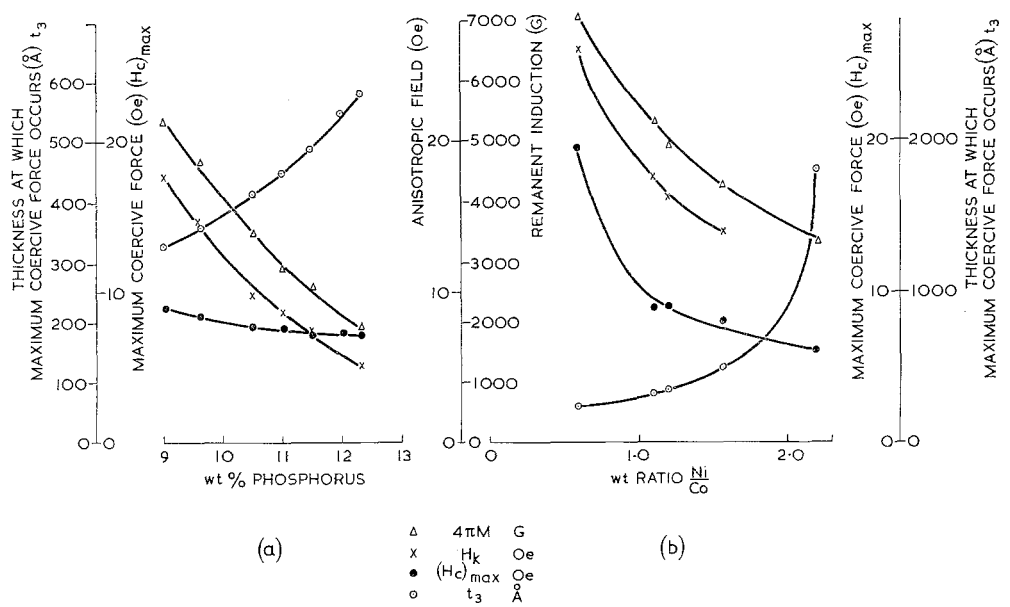

Figure 7 Some magnetic parameters of electroless-deposited Ni-Co-P films. (Note that the right-hand scale for t_3 applies to fig. a and the left-hand scale to fig. b.)

5. Some Applications of the Monitoring System

5.1. The Control of the Magnetic Parameters for Storage Elements

The operation of a thin magnetic film as a storage element in a "word-organised" computer system requires the application of two field pulses: one applied along the macroscopic easy axis, which just exceeds the field level required to overcome the dispersion and the skew of the direction of the local easy axis of magnetisation, but less than the coercivity, H_c; the other a field pulse in the hard direction exceeding the anisotropy field, H_k, and sufficiently large to change the state of magnetisation. For economic reasons the value of H_k needs to be as low as possible so that low drive currents can be used. In some systems the value of the ratio of H_c/H_k is also important and must have a precise value equal to or less than unity. H_k is dependent on chemical composition only, for a particular deposition process, and H_c on the chemical composition and film thickness; therefore, coercive force monitoring during deposition proves very useful in arriving at a particular value of this ratio. Fig. 7 shows the variation of t_3, $(H_c)_{max}$, H_k and remanent induction, B_R, as a function of composition. It shows that H_k decreases for increasing nickel and phosphorus contents. However, films with a nickel/cobalt ratio in excess of 1.2 cannot be used since the dispersion of the easy axis becomes too large (i.e. greater than 5°). Therefore, a composition must be chosen with the ratio less than 1.2 which gives a low value of H_k and low dispersion. By observing the coercive force during deposition, the film may be removed from the bath when the required ratio of H_c/H_k is achieved.

The chemical composition of the film can be assessed to a reasonable degree of accuracy by continually monitoring the values of t_3 and $(H_c)_{max}$ and comparing these values with those previously obtained, as in fig. 7. The bath may be chemically modified to maintain these parameters. This saves considerable time as it avoids the need for accurate chemical analysis.

The uniformity of the magnetic parameters for computer storage elements must come within specified tolerances. Electroless films with nickel/cobalt ratios between 0.6 to 1.1 have skew angles less than $\frac{1}{2}°$ and dispersion of the easy axis less than 3°. The effect of dispersion on the easy axis coercive force can, therefore, be said to be small. However, some electroless films suffer from thickness irregularities up to $\pm$ 100 Å due to non-uniform activation and other causes. Therefore, variations in coercivity will exist over the whole film area. It was shown that the shape of the statistical frequency distribution of coercive force over the whole film was very similar to the shape of the voltage field transients (see fig. 4). The uniformity of the coercive force could therefore be derived from the width of the voltage field function at an arbitrary voltage level, so that the coercive force distribution could be estimated during deposition. This, again, can save considerable time in measuring the uniformity.

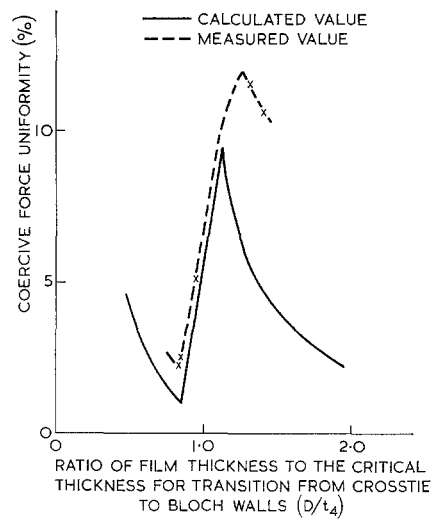

Figure 8 Coercive force uniformity of electroless-deposited Ni-Co-P films.

Fig. 8 shows measured values of coercive force uniformity as a function of film thickness for a film with a nickel/cobalt ratio of 0.9 and phosphorus content of 10.5 wt%. The same figure also shows the calculated values of the coercive force uniformity derived from the coercive force/thickness relationship. These values were calculated by assuming that film thickness variations of $\pm$ 100 Å were the primary cause of any irregularities. Good agreement between the measured and calculated results is obtained; the measured irregularities in coercive force being slightly greater than that calculated, particularly in the Bloch wall region. This result does show that electroless films with a slow rate of change of coercive force with thickness in the range between t_3 and t_4 have extremely uniform co-

Substrate a

Substrate b

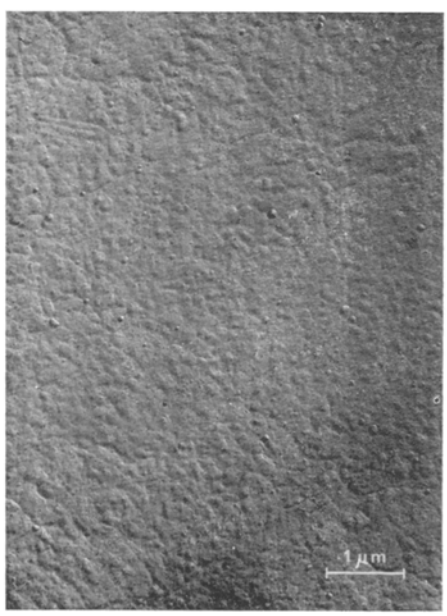

Substrate c

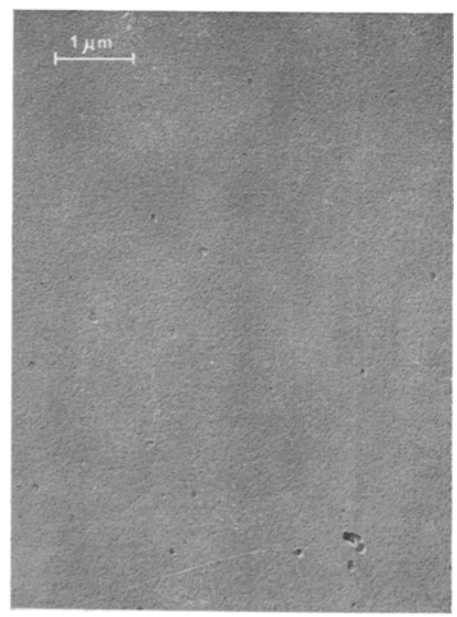

Substrate d

Figure 9 Electron micrographs of treated copper substrates. Substrate a electroformed replica of roller-polished stainless steel. (Talysurf indicates ridges of 1000 Å and variation on average of ±400Å.) Substrate b chemically etched. (Talysurf indicates average variation ±2000 Å.) Substrate c electropolished. (Talysurf indicates average variation ±300 Å.) Substrate d bright-plated. (Talysurf indicates variation < ±50 Å.)

ercivities and measured values of uniformity better than $\pm 2\%$ are obtained.

5.2. Surface Roughness Assessment

Lloyd and Smith [17] have divided the roughness of substrates into three types: firstly those in which the roughness is periodic, with a wavelength large compared to the domain wall width; secondly, those with wavelength of the order of size of a domain wall; and thirdly, surfaces with roughness large compared to the film thickness. For permalloy films with thicknesses in the Bloch wall region, their results obey the general expression

$$H_c = CD^n \qquad (13)$$

where D is the film thickness and C and n are constants dependent on the type and extent of the roughness. They showed that the exponent, n, was dependent on the degree of roughness for the first two roughness types but independent for the third kind. The third kind of roughness was produced by unidirectional polishing and resulted in two effects; one to align the magnetisation along the polishing direction, and secondly to increase the value of the constant of proportionality in the above expression.

These effects are very important when electroplating magnetic films with a uniform coercive force. The uniformity will be improved if variations in thickness have a minimum effect on the coercive force. The relation of coercive force to thickness for films with different types of roughness is therefore of interest.

Three types of electroformed copper substrate surfaces were chosen for experimental purposes. Electron micrographs of these surfaces are reproduced in fig. 9, together with roughness measurements made by means of a Talysurf. The unpolished electroformed copper surface, substrate a, was of the third type given by Lloyd *et al*, in which ridges 1000 Å to 1500 Å high occurred corresponding to polishing lines in the former. The roughness between the ridges was roughly ± 400 Å. When Ni–Co–P was deposited onto this substrate the magnetisation was always aligned along the direction of the ridges and was independent of the direction of the magnetic aligning field. (In the following roughness experiments, the aligning field was always applied in the same direction as the ridges.) The second surface, substrate b, was chemically polished (using Phosbrite 184, Albright and Wilson) and was devoid of ridges but had a patchwork surface of rough and smooth areas. The rough parts were of the second type of roughness and etched pits were also present over the surface. The electropolished surface, substrate c, was of the first type of roughness. The fourth type of surface, substrate d, was bright electroplated (using Pyrobrite, Albright and Wilson) and was of the second type of roughness but with a much smaller amplitude than that of substrate b.

The same Ni–Co–P alloy was electroless deposited onto all the copper surfaces and the coercive force monitored with respect to film thickness. The coercive force/thickness relationships for three of the substrates are given in fig. 10 (the substrate d was identical to substrate c), together with the relationship for deposition onto glass.

For this particular alloy when deposited onto glass, the value of t_4 is approximately 1500 Å. The substrates should, therefore, be compared in the region of thickness above this value since the wall structure is more complex below it. Fig. 10 shows that the highest coercive force for a particular thickness is obtained on substrate b, and that substrate c gives approximately the same value as for the film deposited onto glass. This result is expected because the surface of substrate c will only slightly affect the Bloch wall energy, whereas for the surface of substrate b, which has a periodic roughness of a wavelength comparable to the domain wall width, the Bloch wall energy will be considerably increased. The constant, C, in equation 13 for the range of thickness above 1500 Å has the highest value for substrate b and the lowest for substrate c and the exponent n in the expression is the same for both substrates a and c but higher for b.

For thicknesses below 1500 Å the relationships are different. A closer study of the region around the transition was made by depositing an alloy of higher saturation magnetisation. This is shown in the insert of fig. 10. The substrate a was used and compared with plating onto glass. The result shows that the relationship is distinctly different in the region below t_4 and the value of t_4 is slightly increased.

In conclusion, from observations of the coercive force/thickness relationship of different alloys plated on to various surfaces, the best range of thickness for the required coercive force uniformity may be chosen.

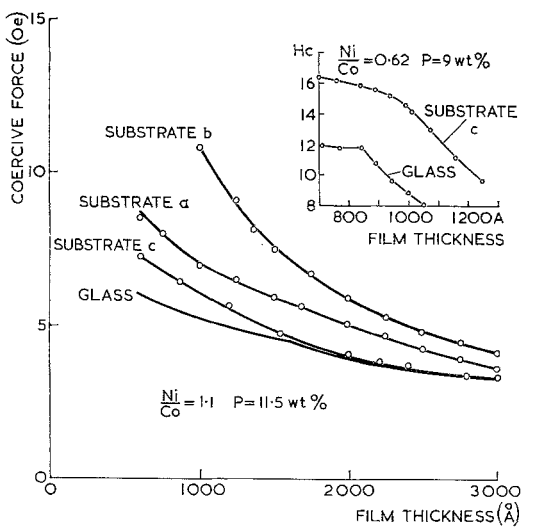

Figure 10 Domain wall coercive force as a function of film thickness for different substrate surfaces.

5.3. The Coupling Phenomena between Two Ferromagnetic Films

Bruyère *et al* [4, 5] have observed an apparently new type of coupling between two uniaxial ferromagnetic thin films of differing coercivity separated by a third metallic non-magnetic thin film. This coupling tends to produce parallel alignment of the directions of magnetisation of the two ferromagnetic films. The coupling appeared to be dependent upon the intermediate material, its thickness and the nature of the ferromagnetic films. These interactions were observed for intermediate thicknesses up to 300 Å. The measured surface energy of the coupling was of the order of 0.1 erg/cm^2. Néel [18] has calculated on the basis of surface roughness that the coupling should be of the order of 0.01 erg/cm^2 for magnetostatic interaction due to the surface topography of an intermediate layer.

The authors have electroplated three-layer films including an intermediate layer of bright-plated copper (Pyrobrite). Electropolished planar substrates measuring 10 by 7.5 cm and bright copper-plated 20 swg wire substrates were used. The two ferromagnetic layers consisted of Ni–Fe–P (80.0/19.3/0.7) and of Ni–Fe–Co (18.8/4.0/77.2); the thicknesses were adjusted so that the magnetic flux from the two layers was the same. The ratio of the coercive force of the two layers was approximately 8:1. Tracings of photographs of easy axis B/H loops of planar films for intermediate film thicknesses of zero, 50 Å, 100 Å, 150 Å, 200 Å, 300 Å, 1000 Å and 2500 Å are shown in fig. 11. (The external demagnetising field of these films is very small and its coupling effect can be neglected.)

The lower set of diagrams in fig. 11 shows that, when the composite film is saturated, the hysteresis loop shape is critically dependent on the thickness of the intermediate copper layer. For the thick intermediate layers (numbers 1 and 2 of fig. 11), the hysteresis loop is simply the summation of the hysteresis loops of the two individual layers. When the copper layer has a thickness of between 150 and 300 Å (numbers 3, 4 and 5 of fig. 11), the hysteresis loop is approximately the same shape as that for the thicker copper layers. However, the coercivity of the Ni–Fe–P layer is slightly increased and that of the Ni–Fe–Co layer is slightly decreased. For copper thicknesses less than or equal to 100 Å (numbers 7, 6 and 8), a normal hysteresis loop is observed with a coercive force approximately equal to the mean coercive force of the two individual films. The appearance of this normal hysteresis loop shows that complete parallel coupling occurs between the two ferromagnetic layers. When smaller drive fields are applied to the composite film such that only half the total flux is reversed, the films with negligible coupling show a hysteresis loop characteristic of the lower-coercive-force Ni–Fe–P film. However, for those films which are coupled, the low field hysteresis loop is distinctly different and an approximately zero remanent induction is obtained. This condition also occurs when the two magnetic layers have no copper layer between them, even though precautions against oxide formation were taken by keeping the films wet during transference between plating baths; however, it must be assumed that a layer of some sort is present in this case. The critical thickness for coupling can be measured more accurately by monitoring the coercive force/thickness relationship during deposition. At first the coercive force/thickness relationship of single layer films of Ni–Fe–P and Ni–Fe–Co were measured and are shown in fig. 12. The composition of these two films was kept constant throughout. The Ni–Fe–P low-coercive-force layer was deposited first, followed by the copper layer. The third layer was then deposited and the coercive force/thickness relationship of this layer monitored during deposition, these results being shown in fig. 12.

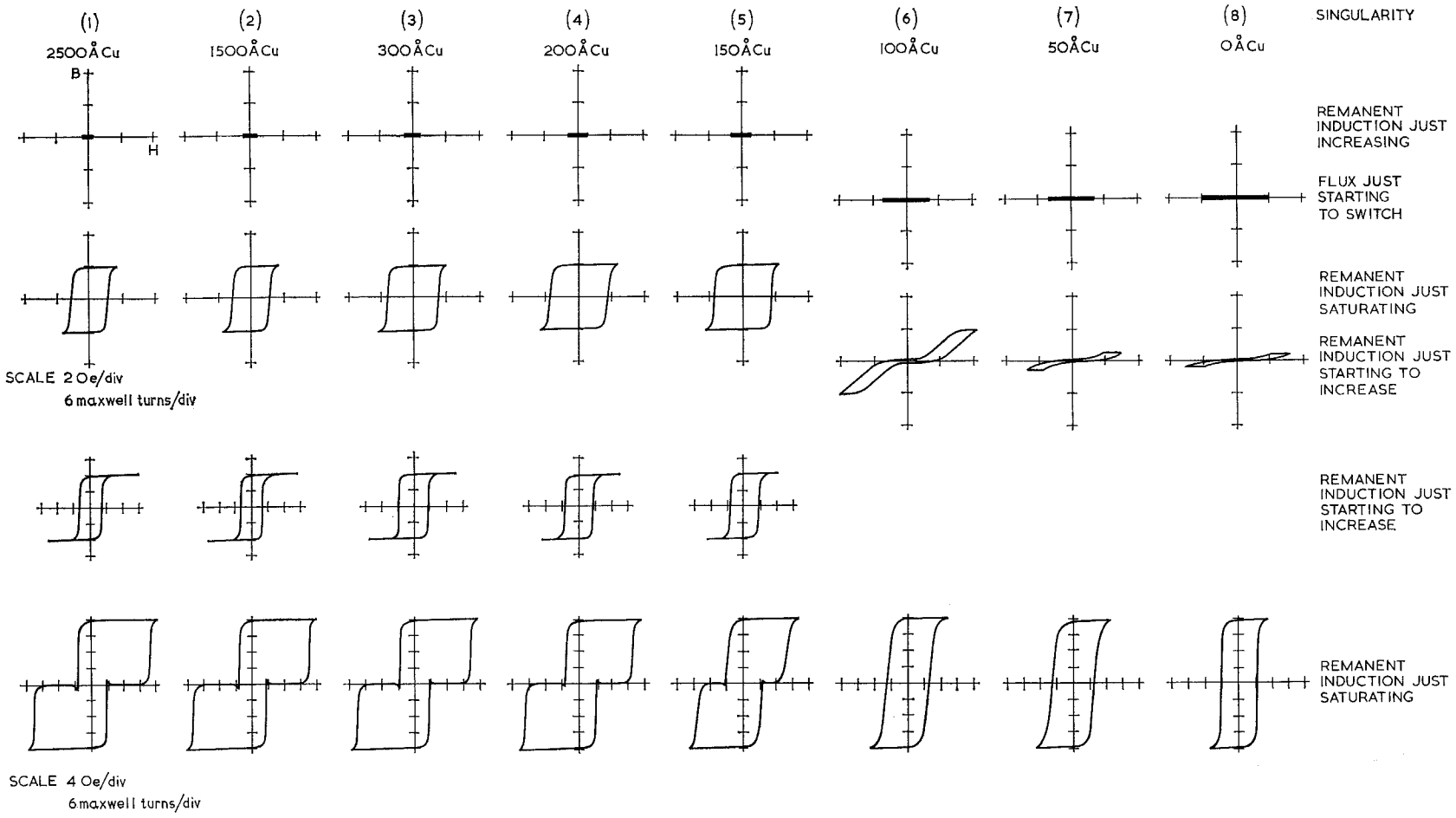

Figure 11 Hysteresis loops of electroplated double layer ferromagnetic film showing coupling phenomena.

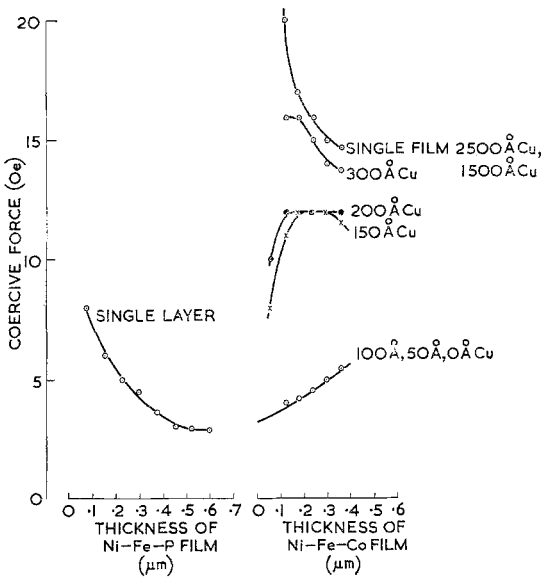

Figure 12 Coupling phenomena of double layer ferromagnetic films as a function of the intermediate copper film thickness.

The relationship for thick intermediate copper layers (1000 Å and 2500 Å) is the same as for the Ni–Fe–Co high-coercivity-force film alone. When the intermediate copper thickness was reduced to 300 Å the coercive force was found to be lower. For lower copper thicknesses (200 and 150 Å) the level of coercive force was reduced still further and the form variation was considerably altered. At still lower copper thicknesses, at 100 Å and below, the coercive force increased with increasing film thickness from the final value of the Ni–Fe–P film. This would be expected if an averaging effect of the saturation magnetisation and exchange constant took place. The figure therefore shows that some coupling between the two ferromagnetic layers exists at intermediate thicknesses as high as 300 Å, and that complete coupling occurs at thicknesses below 100 Å.

The surface topography of the intermediate layer of copper has a roughness of the same order as that assumed by Néel [18] in his calculations of the exchange energy coupling. However, island growth may still exist at this thickness. (This also applies to the films of Bruyère *et al* [4, 5].) In conclusion, films have been electroplated which show a similar coupling phenomenon to that observed by Bruyère *et al* [4, 5], and coercive force monitoring serves to show that some coupling between the two ferromagnetic layers exists even with intermediate copper thicknesses as great as 300 Å.

6. Conclusions

The experimental method described permits the coercive force/thickness relationship to be reliably determined, and avoids the problems encountered by previous techniques. The experimental values of the critical thicknesses, t_3 and t_4, at which coercive force anomalies occur, allow the determination of the exchange constant for the magnetic material. Coercive force monitoring during deposition enables films to be prepared with the desired magnetic parameters for computer storage systems. The method is also a useful tool for determining the critical thickness of an intermediate, non-magnetic layer separating two ferromagnetic thin films.

Acknowledgements

Thanks are due to The Plessey Co Ltd and the Ministry of Aviation for permission to publish this paper. The authors also wish to thank R. J. Heritage for many helpful discussions.

References

1. P. J. HULYER, Mullard Research Report 505 (1964).
2. S. METHFESSEL, S. MIDDELHOEK and H. THOMAS, *IBM J. Res. Dev.* **4** (1960) 96.
3. *Idem, J. Appl. Phys. Supp.* 31 (1960) 302.
4. J. BRUYÈRE, O. MASSENET, R. MONTMORY and L. NÉEL, *Proc. Inter. Conf. on Non Linear Magnetics* **16-1-2** (1964).
5. J. BRUYÈRE, J. DEVENYI, O. MASSENET, R. MONTMORY and L. NÉEL, *Int. Conf. on Magnetism* (1964) 789.
6. L. NÉEL, *Compt. Rend.* **241** (1955) 533.
7. S. MIDDELHOEK, *J. Appl. Phys. Supp.* 34 (1963) 1054.
8. L. NÉEL, *J. Phys. Radium* **17** (1956) 250.
9. S. MIDDELHOEK, Ph.D. Thesis, Amsterdam (1961).
10. H. D. RICHARDS, to be published in *Brit. J. Appl. Phys.*
11. R. J. HERITAGE and M. I. WALKER, *J. Electronics and Control* **7** (1960) 542.
12. C. A. NEUGEBAUER, *Proc. Inter. Conf. on Single Crystal Films* (1963) 365.
13. R. KIMURA and H. NOSE, *J. Phys. Soc. Japan, Supp.* B1 **17** (1962) 607.
14. Z. FRAIT and M. ONDRIS, *Czech. J. Phys.* **121** (1961) 715.
15. C. KITTEL, *Rev. Mod. Phys.* **21** (1949) 541.
16. M. HANSEN, "Constitution of Binary Alloys" (McGraw-Hill, 1958) p. 486.
17. J. LLOYD and R. SMITH, *J. Appl. Phys. Supp.* 30
18. (1959) 274.
L. NÉEL, *C R Acad. Sci. (France)* **255** (1962) 1676.